Medicine®

OBSERVATIONAL STUDY

OPEN

Evaluation of a Simplified Intravoxel Incoherent Motion (IVIM) Analysis of Diffusion-Weighted Imaging for Prediction of Tumor Size Changes and Imaging Response in Breast Cancer Liver Metastases Undergoing Radioembolization

A Retrospective Single Center Analysis

Claus C. Pieper, MD, Alois M. Sprinkart, MSc, Carsten Meyer, MD, Roy König, MD, Hans H. Schild, MD, Guido M. Kukuk, MD, and Petra Mürtz, PhD

Abstract: To investigate the value of a simplified intravoxel incoherent motion (IVIM) analysis for evaluation of therapy-induced tumor changes and response of breast cancer liver metastases (mBRC) undergoing radioembolization.

In 21 females (mean age 54 years, range 43–72) with mBRC tumor size changes and response evaluation criteria in solid tumors (RECIST) response to 26 primary radioembolization procedures were analyzed. Standard 1.5-T liver magnetic resonance imaging including respiratory-gated diffusion-weighted imaging (DWI) with b0 = 0 s/mm^2, b1 = 50 s/mm^2, b2 = 800 s/mm^2 before and 6 weeks after each treatment was performed. In addition to the apparent diffusion coefficient (ADC)(0,800), the estimated diffusion coefficient D′ and the perfusion fraction f′ were determined using a simplified IVIM approach. For each radioembolization, the 2 largest treated metastases (if available) were analyzed. Lesions were categorized according to size changes into group A (reduction of longest diameter [LD]) and group B (LD increase) after 3 months. Radioembolization procedures were further categorized into ''response'' (partial response and stable disease) and ''nonresponse'' (progressive disease) according to RECIST after 3 months. ADC and D′ are given in 10^{-6} mm^2/s.

Forty-five metastases were analyzed. Thirty-two lesions were categorized as A; 13 as B. Before therapy, group A lesions showed significantly larger f′-values than B ($P = 0.001$), but ADC(0,800) and D′ did not differ. After therapy, in group A lesions the ADC(0,800)- and D′-values increased and f′ decreased ($P < 0.0001$); in contrast in group B lesions f′ increased ($P = 0.001$). Groups could be differentiated by preinterventional f′ and by changes of D′ and f′ between pre and postinterventional imaging (area under the curve [AUC] of 0.903, 0.747 and 1.0, respectively).

Preinterventional parameters did not differ between responders and nonresponders according to RECIST. ADC(0,800)- and D′-values showed a larger increase in responders compared with nonresponders ($P = 0.013$ and $P = 0.001$, respectively). After therapy f′-values decreased significantly in responders ($P = 0.001$). Good to excellent prediction of long-term RECIST response was possible by therapy-induced changes in LD, D′, and f′ (AUC 0.903, 0.879, and 0.867, respectively).

A simplified IVIM model-based analysis of early post-treatment DWI can deliver additional information on tumor size changes and long-term RECIST response after radioembolization of mBRC. The estimated perfusion fraction f′ is better suited for response assessment than the conventional ADC(0,800) or D′. This can be useful to guide further treatment strategy.

(*Medicine* 95(14):e3275)

Abbreviations: ADC = apparent diffusion coefficient, BSA = body-surface-area, CR = complete response, CT = computed tomography, D = true diffusion coefficient, D∗ = pseudo-diffusion coefficient, D′ = estimated diffusion coefficient, DWI = diffusion-weighted imaging, f = perfusion fraction, f′ = estimated perfusion fraction, FDG = fluorodeoxyglucose, IVIM = intravoxel incoherent motion, LD = longest diameter, mBRC = metastasized breast cancer, MRI = magnetic resonance imaging, PD = progressive disease, PET = positron-emission tomography, PR = partial response, RECIST = response evaluation criteria in solid tumors, ROC = receiver operating characteristic, ROI = region of interest, SD = stable disease, SPECT/CT = single photon emission computed tomography/computed tomography, Tc99m-MAA = Technetium-99m-macroaggregated-albumin.

INTRODUCTION

There are several imaging-based approaches to assess tumor response after therapy. Morphological response evaluation (e.g., Response Evaluation Criteria in Solid Tumors, RECIST)[1] alone has limitations as changes in tumor size may occur late after treatment.[1–8] Functional imaging modalities (e.g., mRECIST, diffusion-weighted magnetic resonance imaging [MRI], positron-emission tomography [PET], perfusion-computed tomography [CT]) have therefore been proposed to improve the accuracy of early response assessment.[2,9–12]

Diffusion-weighted imaging (DWI) may be useful for early tumor response evaluation by providing information on alterations of tissue cellularity, extracellular space tortuosity, and integrity of cell membranes (e.g., in developing necrosis) without application of contrast agents or radiation exposure.[3,13–18] To perform quantitative analysis of DWI data, conventionally an apparent diffusion coefficient (ADC) is determined with b-values

Editor: Li Gong.
Received: January 8, 2016; revised: February 10, 2016; accepted: March 4, 2016.
From the Department of Radiology, University of Bonn, Bonn, Germany.
Correspondence: Claus C. Pieper, Department of Radiology, University of Bonn, Sigmund-Freud-Straße 25, 53105 Bonn, Germany (e-mail: claus.christian.pieper@ukb.uni-bonn.de).
CM is a consultant for SIRTEX Medical, PharmaCept, and GoreMedical. GMK has received payment for lectures from Philips Healthcare. For the remaining authors no conflicts of interest were declared.
The authors have no funding to disclose.
Supplemental Digital Content is available for this article.

ISSN: 0025-7974
DOI: 10.1097/MD.0000000000003275

between 0 and 500 to 1000 s/mm^2 assuming mono-exponential behavior of signal intensity depending on the b-values.[3,14] An increase of the ADC is related to therapy-induced necrosis.[3,13,14,16] However, DWI is sensitive not only to molecular diffusion, but also to pseudo-random movements, such as blood flow in the capillary network, leading to additional signal attenuation at low b-values.[15,16] For DWI acquired with more than 2 b-values, a refined analysis based on the intravoxel incoherent motion (IVIM) theory can be performed.[19] By assuming bi-exponential behavior of signal intensity, diffusion and perfusion influences can be separated, yielding an estimation of the true diffusion coefficient D, the pseudo-diffusion coefficient D* and the perfusion fraction f.[20] There is first evidence that IVIM model-based analysis can improve response assessment of liver tumors.[21,22]

In diffuse liver disease, blood flow velocity (reflected by D*) was found to be altered so that research recently focused on an accurate determination of D* using nonlinear least-squares fit procedures with numerous b-values (typically $\geq$8).[23–28] However, in malignant liver lesions, IVIM analysis using fitting procedures is challenging due to weak bi-exponential behavior of signal decay and/or a low IVIM effect (low D*- and f-values) leading to fitting failures and poor reproducibility.[23,29–33] Furthermore, the acquisition of numerous b-values requires long acquisition times (about 10 min).[24,25,34] Thus, for evaluation of IVIM parameters in malignant lesions in a clinical setting, an alternative IVIM approach has to be developed, that yields a numerically stable estimation of at least D and f also in cases of low D*- and f-values. Of note, such estimates may not necessarily provide an accurate quantification of the true IVIM parameters, but may serve as empirical biomarkers for assessment of therapy-induced changes. Furthermore, short acquisition times and a voxel-wise analysis providing parameter maps are important for clinical application.

The aim of our study was to investigate the value of a simplified IVIM analysis for evaluation of therapy-induced changes and tumor response in patients undergoing radioembolization of breast cancer liver metastases (mBRC).

MATERIALS AND METHODS

Patients

Patients undergoing radioembolization for liver-dominant mBRC between July 2006 and February 2015 were identified in the clinical database. Indication for radioembolization was discussed in interdisciplinary tumor boards. Approval of the local institutional review board of the university hospital of Bonn for this retrospective study was obtained; patient consent was waived.

Inclusion criteria were primary resin-based radioembolization (i.e., of previously radioembolization-naive tissue) performed at our institution, accessible procedural/clinical data, and availability of MRI before and after intervention including DWI without motion artifacts. Patients with incomplete imaging data were excluded.

Radioembolization

Radioembolization was performed according to clinical standards.[35,36] Planning-angiography was done to evaluate vascular liver anatomy. After injection of Technetium-99m-macroaggregated-albumin (Tc99m-MAA) into the target arteries, SPECT/CT was performed to exclude extrahepatic Tc99m-MAA deposition, to quantify pulmonary shunting, and to evaluate tumor-to-nontumor uptake-ratio. The prescribed activity for radioembolization was calculated using the body-surface-area (BSA) method in compliance with international consensus guidelines.[35] For radioembolization, a microcatheter (e.g., Renegade, Boston Scientific, Natick, MA) was positioned in the selected artery, with careful injection of small amounts of a suspension of resin spheres (SIR spheres, Sirtex Medical Limited, North Sydney, Australia) in sterile water and repetitive contrast injections. In accordance with local regulations, patients were admitted to a special ward for 2 days postinterventionally.

Pre and Postinterventional Imaging

Patients underwent MRI examinations of the liver before (baseline), 4 to 6 weeks (first/short-term follow-up) and 3 months (second/long-term follow-up; if possible) after radioembolization. MR examinations were performed on a clinical 1.5-T MRI scanner (Philips Healthcare, Best, The Netherlands; Gyroscan Intera and Ingenia; gradient system: maximum amplitude of 30 and 45 mT/m, respectively, maximum slew rate of 150 and 200 T/m per s, respectively, in supine position). A commercially available phased-array surface coil was used for signal reception. Each patient was examined on the same MR scanner both pre and postinterventionally. The standardized imaging protocol comprised a respiratory-triggered single-shot spin-echo echo-planar DWI sequence (Supplemental Table 1, http://links.lww.com/MD/A875) with motion-probing gradients in 3 orthogonal directions and 3 b-values (b0 = 0 s/mm^2, b1 = 50 s/mm^2, b2 = 800 s/mm^2), acquired prior to contrast agent injection. Diffusion-weighted images were reconstructed on the MRI system. Additionally, a T2-weighted sequence with and without fat suppression, a T1-weighted sequence, and a T1-weighted dynamic contrast-enhanced sequence were acquired.

Image Analysis

Image analyses were performed in consensus by a radiologist with more than 4 years of imaging and interventional experience, and a physicist with more than 17 years of experience in DWI, blinded to baseline and follow-up information. Within the treated portion of the liver, the largest and second largest metastases (if present) with a diameter of $\geq$1 cm were selected.

For each included metastasis, the change of tumor size was evaluated using the longest diameter (LD) on morphological images of the first and second (if available) follow-up examinations in comparison to baseline MRI. Furthermore, for each treated liver area imaging response was determined on first and second follow-up examinations using RECIST criteria.[1]

IVIM analysis was performed for baseline and first follow-up MRI. A hand-drawn region of interest (ROI) was placed within a central slice of each metastasis, without noticeable motion artifacts, pixel misalignments, or susceptibility artifacts. Blood vessels were avoided. All ROIs were drawn on the diffusion-weighted image with b = 800 s/mm^2 or b = 50 s/mm^2 excluding areas close to the rim to avoid partial volume effects. The position of the ROI was visually cross-checked between all DWI images and was then copied into the parameter maps. For each ROI, the mean parameter value and standard deviation were determined.

The IVIM model-derived true diffusion coefficient D and perfusion fraction f were estimated as D′ and f′ by using a simplified approach as originally introduced by Le Bihan et al[19] and recently applied to abdominal imaging for b-values b0 = 0

s/mm^2, b1 = 50 s/mm^2, and b2 = 800 s/mm^2 with[37,38]

$$D' = ADC(50, 800) = (\ln(S(b1)) - \ln(S(b2)))/(b2 - b1) \quad (1)$$

and

$$f' = 1 - S(b1)/(S(0)) \cdot \exp(-b1 \cdot ADC(50, 800)). \quad (2)$$

S(b) and S(0) are the signal intensities with and without motion-probing gradients.

The ADC(0,800) was also calculated:

$$ADC(0, 800) = (\ln(S(b0)) - \ln(S(b2)))/(b2 - b0). \quad (3)$$

Parameter maps were generated by voxel-wise calculation of ADC(0,800), D′ and f′ using MATLAB (Math Works, Natick, MA).

Statistical Analysis and Definitions

Statistics were performed using commercially available software (SPSS, version 22.0, IBM, Armonk, NY). Normal distribution was assessed using Q–Q plots.

Association of IVIM Parameters With Long-Term Tumor Size Changes

Analysis was performed on a lesion basis. Metastases were categorized into 2 groups according to long-term tumor size changes:

- Group A (tumor-shrinkage): reduced LD on second follow-up; regardless of changes on first follow-up.
- Group B (tumor-growth): increased LD on second follow-up (even if metastases showed initial shrinkage on first follow-up). In patients showing growth on first follow-up who did not survive or were too ill to attend second follow-up, metastases were also categorized as B.

A 2-sided Student *t* test was used to test statistical significance ($P < 0.05$) of differences in IVIM parameters between groups A and B (independent samples, variance analysis by Levene test) and between pre and postinterventional values within the respective groups on a lesion basis (paired samples). Receiver operating characteristic (ROC) analysis was performed to calculate sensitivity, specificity, and accuracy of IVIM parameters for prediction of tumor size changes classified as described above.

Association of IVIM Parameters and Short-Term Tumor Size Changes With Long-Term RECIST Response

Analysis was performed on a radioembolization procedure basis. Data were categorized according to long-term RECIST response of the treated liver area:

- Responder: complete/partial response (CR/PR) and stable disease (SD) on second follow-up, regardless of RECIST response on first follow-up.
- Nonresponder: progressive disease (PD); note: patients showing PD on first follow-up who did not survive or were incapable to undergo second follow-up were also categorized as ''nonresponders.''

For this analysis the IVIM parameter values of the largest and second-largest metastasis were averaged with weights according to ROI size after proving that no significant differences existed between both metastases. Tumor size changes of the 2 metastases were also averaged. For IVIM parameters and short-term tumor size changes, differences between responders and nonresponders were analyzed using a Student *t* test. ROC analysis was performed to investigate the value of IVIM parameters and short-term LD changes for prediction of long-term RECIST response.

RESULTS

Patient Characteristics

Out of 44 treated patients, 21 fulfilled the inclusion criteria (mean age 54 years, range 43–72 years; Figure 1). In these patients, 26 primary radioembolization procedures were analyzed. Mean Y90 activity was 1.3 (SD 0.7, range 0.33–2.90) GBq (group A: 1.2, range 0.4–2.9 GBq and group B: 1.4, range 0.33–2.2 GBq).

While a first follow-up MRI was performed in all 21 patients, a second follow-up was available in 15/21 patients. Of 21 patients, 5 did not survive until second follow-up MRI; 1 patient was incapable to undergo second follow-up due to the severe illness. Mean time between pretherapeutic MRI and therapy was 21 ± 21 days (1–71 days), between therapy and first follow-up 34 ± 4 days (28–42 days) and between therapy and second follow-up MRI 101 ± 20 days (76–161 days). Median overall survival after the first radioembolization was 151 days (46–1647 days). Two patients were still alive at the date of analysis (147 and 227 days after radioembolization).

Association of IVIM Parameters With Long-Term Tumor Size Changes

Overall 45 metastases were analyzed. Thirty-two metastases were assigned to group A with a mean LD change of −28% (−61% to 0%) and −44% (−80% to −8%) on first and

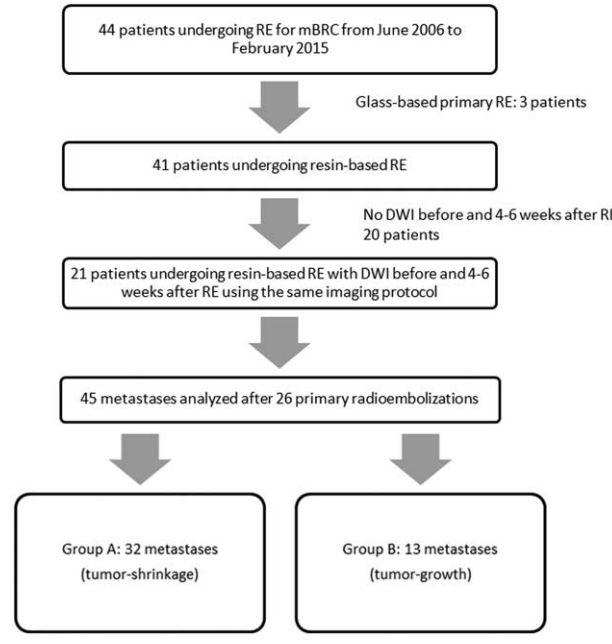

FIGURE 1. Flow chart showing the total number of patients undergoing radioembolization (RE) of breast cancer liver metastases (mBRC) during the study period and excluded data.

TABLE 1. Results of Metastasis-Based Comparison of Pre- and Post-Treatment Measurements

	Pretreatment	Post-Treatment (First Follow-Up)	*P* Value
All metastases (n = 45)			
LD, mm	38.5 ± 21.5	35.5 ± 25.0	>0.0500
ADC (0,800), 10^{-6} mm^2/s	1200.0 ± 271.5	1585.1 ± 343.3	**<0.0001**
D′, 10^{-6} mm^2/s	1124.4 ± 257.4	1573.0 ± 368.1	**<0.0001**
f′	0.0712 ± 0.0430	0.0484 ± 0.0370	**0.0070**
Group A (long-term tumor shrinkage) (n = 32)			
LD, mm	38.1 ± 21.8	28.7 ± 20.0	**<0.0001**
ADC (0,800), 10^{-6} mm^2/s	1198.2 ± 306.5	1654.4 ± 331.5	**<0.0001**
D′, 10^{-6} mm^2/s	1097.2 ± 284.9	1673.6 ± 327.2	**<0.0001**
f′	0.0843 ± 0.0423	0.0351 ± 0.0250	**<0.0001**
Group B (long-term tumor growth) (n = 13)			
LD, mm	39.2 ± 21.4	52.2 ± 28.9	**0.0100**
ADC (0,800), 10^{-6} mm^2/s	1204.6 ± 166.0	1414.4 ± 322.2	0.0910
D′, 10^{-6} mm^2/s	1191.4 ± 162.6	1325.7 ± 356.5	0.2690
f′	0.0391 ± 0.0248	0.0812 ± 0.0422	**0.0010**

Data are given as mean and standard deviation over the region of interest values. $P < 0.05$ considered statistically significant (2-sided Student *t* test for paired samples).

ADC = apparent diffusion coefficient, D′ = estimated true diffusion coefficient (i.e., ADC(50,800)), f′ = estimated perfusion fraction, LD = longest diameter.

Significant test results given in bold.

second follow-up, respectively, compared with baseline. Thirteen metastases were assigned to group B: on first follow-up, tumor size had increased in 12 cases and decreased in 1 case (mean LD change: 35% [−31% to 135%]); on second follow up, the latter case showed considerable increase of tumor size of 25% compared with baseline. Beside this case, a second follow-up was available only for 1 other patient of group B showing a further increase of tumor size (from 14% to 100%).

Mean ROI sizes for the largest and second-largest metastases at baseline were 881 ± 925 and 602 ± 546 mm^2, respectively, and 816 ± 895 and 476 ± 459 mm^2, respectively, on first follow-up.

In group A (tumor-shrinkage), ADC(0,800) and D′ increased significantly (both $P < 0.0001$) while f′ decreased ($P < 0.0001$) after therapy.

In group B (tumor-growth), no significant changes were found for ADC(0,800) or D′, while f′ increased significantly ($P = 0.001$; Table 1).

Group comparison for pretreatment values revealed significantly larger f′-values in group A than in B (0.0843 ± 0.0420 vs 0.0391 ± 0.0248, $P = 0.001$), while ADC(0,800) and D′ did not differ significantly. After therapy, significantly higher ADC(0,800)- and D′-values ($P = 0.032$ and $P = 0.003$, respectively) and significantly lower f′-values ($P = 0.002$) were found for group A compared with B.

The calculated differences of post and pretreatment values showed a significantly larger increase of D′ and a larger decrease of f′ in group A compared with B ($P = 0.003$ and $P < 0.0001$, respectively) while the differences of ADC(0,800)-values were not significant (Table 2).

ROC analysis (Table 3) showed that both groups were excellently discriminated by changes in f′ and by pretherapeutical f′-values (area under the curve [AUC] of 1.000 and 0.903, respectively). Inferior group differentiation was possible by post-therapeutical values of f′, D′, and ADC(0,800), as well as changes in D′ (AUC of 0.806, 0.739, 0.696, and 0.747, respectively). Groups were not significantly discriminated by changes in ADC(0,800) or pretherapeutical ADC(0,800)- and D′-values.

Association of IVIM Parameters and Short-Term Tumor Size Changes With Long-Term RECIST Response

''Response'' according to RECIST was found in 15 radioembolization procedures (10 PR and 5 SD), while ''nonresponse'' was found in 11 (4 with initial SD but PD on second follow-up; 7 with initial PD without ever reaching disease stabilization). In 3 of these cases, response was rated as PD solely on the basis of new metastases.

No significant differences in preinterventional IVIM parameters between responders and nonresponders were found. Postinterventional ADC(0,800)- and D′-values were significantly higher and f′-values were significantly lower in responders compared with nonresponders ($P = 0.02$, $P = 0.002$, and $P = 0.032$, respectively). When analyzing therapy-induced changes, ADC(0,800)- and D′-values showed a significantly larger increase in responders compared with nonresponders ($P = 0.013$ and $P = 0.001$, respectively). Changes in f′ differed significantly between the groups ($P = 0.001$) with decreasing values in responders and increasing values in nonresponders. Short-term tumor size changes also differed between responders and nonresponders ($P = 0.001$). Details are given in Table 4.

Long-term RECIST response were well predicted by therapy-induced changes of D′, f′, and LD. Inferior, but still significant discrimination was also possible by postinterventional values of D′, f′, and ADC(0,800) as well as therapy induced changes of ADC(0,800). Preinterventional IVIM parameter values did not significantly differentiate responders from nonresponders. f′ changes had the highest accuracy for response discrimination. Details are given in Tables 3 and Supplemental Table 2, http://links.lww.com/MD/A875.

Examples of DWI measurements are shown in Supplemental Figure 1, http://links.lww.com/MD/A875.

TABLE 2. Results of Metastasis-Based Group Comparison With Categorization According to Long-Term Tumor Size Changes

	Group A (Tumor Shrinkage; n = 32)	Group B (Tumor Growth; n = 13)	*P* Value
Pretreatment			
ADC (0,800), 10^{-6} mm^2/s	1198.2 ± 306.5	1204.6 ± 166.0	0.9440
D′, 10^{-6} mm^2/s	1097.2 ± 284.9	1191.4 ± 162.6	0.2710
f′	0.0843 ± 0.0423	0.0391 ± 0.0248	**0.0010**
Post-treatment			
ADC (0,800), 10^{-6} mm^2/s	1654.4 ± 331.5	1414.4 ± 322.2	**0.0320**
D′, 10^{-6} mm^2/s	1673.6 ± 327.2	1325.7 ± 356.5	**0.0030**
f′	0.0351 ± 0.0250	0.0812 ± 0.0422	**0.0020**
Absolute differences between pre- and post-treatment values			
ΔADC (0,800), 10^{-6} mm^2/s	467.6 ± 249.1	209.9 ± 411.4	0.0520
ΔD′, 10^{-6} mm^2/s	569.8 ± 134.3	263.4 ± 417.9	**0.0030**
Δf′	−0.0492 ± 0.0343	0.0421 ± 0.0349	**<0.0001**

Data are given as mean and standard deviation over the region of interest values. $P < 0.05$ considered statistically significant (2-sided Student *t* test for independent samples).

ADC = apparent diffusion coefficient, D′ = estimated true diffusion coefficient (i.e., ADC(50,800)), f′ = estimated perfusion fraction.

Significant test results given in bold.

DISCUSSION

IVIM model-based analysis of DWI was introduced as a means to separate the influences of tissue diffusivity and blood flow of the capillary network within a voxel.[19] At low b-values (<100 s/mm^2) perfusion leads to additional signal attenuation so that IVIM analysis can yield information on the amount of microvasculature (perfusion fraction f), blood flow velocity, and vessel architecture (pseudo-diffusion coefficient D*). At higher b-values (>100 s/mm^2) signal attenuation primarily depends on molecular diffusion (true diffusion coefficient D).[20,39] In general, an increase of the ADC can reflect therapy-induced necrosis.[3,11,13,14,16] First studies have already described lower f- and D*-values of malignant liver lesions as compared with normal liver tissue.[29–31,38,40] In tumors, lower f-values correlated with a lower histological microvessel density[41] and with a lower histological vascular area fraction.[42] Blood vessels in malignant tumors also tend to be immature and leaky, thus contributing to a high intralesional interstitial fluid pressure and subsequent slow blood flow,[43,44] which causes low D*-values. Viable tumor tissue showed significantly lower diffusion coefficients D and higher perfusion fractions f than necrotic areas.[45]

IVIM analysis using nonlinear fitting procedures for simultaneous determination of D, D*, and f is time consuming, complex, and challenging: Malignant liver lesions can present with a weak bi-exponential signal decay and/or a low IVIM effect (low D*- and f-values) associated with fitting failures and poor reproducibility.[23,29–33] In this study, we present a simplified IVIM approach as originally introduced by Le Bihan et al.[19] This method enables the determination of an estimated diffusion coefficient D′ and perfusion fraction f′ derived from a low number of b-values with sufficient signal averages. By providing a numerically stable voxel-wise analysis method in combination with short acquisition times of about 3 min, this approach is suitable for a clinical setting, as recent publications on liver and pancreatic lesions have demonstrated.[22,37,38] It is important to note that f′, estimated from b-values of 0, 50, and 800 s/mm^2, is influenced both by f and D*, especially in malignant lesions (flatter slope of the signal decay curve compared with liver tissue).[29–31] Thus, f′ reflects not only the amount of microvasculature but also the blood flow velocity and vessel architecture. To our knowledge there are no studies investigating IVIM analysis for mBRC. However, our results are in concordance with published D- and/or f-values obtained for metastases from other primary cancer,[18,21,31,40,46] although varying methodology of different studies makes a direct comparison difficult.[47,48]

For interpretation of measurement results it is important to note which part of a tumor is actually analyzed. In a study on radioembolization of neuroendocrine liver metastases analyzing the viable part of the metastases, lower pretreatment perfusion sensitive ADC(0,50) with increasing values after therapy identified responders.[21] However, this approach is only applicable if larger areas of necrosis can be readily identified. As we intended to investigate an approach that would also be applicable in clinical routine and mBRC are often heterogenic with small necrotic areas scattered throughout the metastasis, we chose to analyze the whole metastasis to perform an analysis of overall changes in the tumor. Hence, the increase of necrotic tissue considerably contributed to the results of our measurements. Prior to radioembolization, metastases showing long-term size reduction had higher f′-values than growing metastases. This is possibly associated with a higher degree of microvascularization in responding tumors with faster blood flow allowing for a fair distribution of the SIR spheres during radioembolization. Adequate embolization as well as the development of necrotic tissue in responding metastases may then explain the observed drop of f′ and increase in D′ after therapy.[3,22] One additionally has to bear in mind that observed changes in f can partly also be caused by changes in relaxation times (i.e., increase in tissue T2-relaxation time in necrotic areas).[48]

In recent years, efforts have been made to establish the value of conventional DWI analysis both for pretherapeutical prediction of morphological response as well as for early post-therapeutical response assessment. For colorectal and gastric cancer liver metastases, two studies have shown that low pretreatment ADC(100,500), ADC(150,500), and ADC(0,800) values, which may reflect a lack of necrosis, predicted better morphological response to chemotherapy.[46,49] Furthermore a negative correlation between pretreatment ADC values and tumor size

TABLE 3. Results of Receiver Operating Characteristic Analyses for Differentiation Between Groups A and B According to Long-Term Tumor Size Changes as well as for Prediction of Long-Term RECIST Response

	AUC (SE)	*P* Value	Optimum Threshold	Sensitivity, %	Specificity, %	Accuracy, %
Long-term tumor size changes						
Pretreatment						
ADC (0,800), 10^{-6} mm^2/s	0.543* (0.089)	0.665				
D′, 10^{-6} mm^2/s	0.669* (0.085)	0.088				
f′	0.903 (0.053)	**<0.0001**	0.048	87.1	83.3	84.4
Post-treatment						
ADC (0,800), 10^{-6} mm^2/s	0.696 (0.089)	**0.048**	1853	35.5	100	53.3
D′, 10^{-6} mm^2/s	0.739 (0.084)	**0.016**	1816	41.9	100	57.8
f′	0.806* (0.071)	**0.002**	0.040	67.7	91.7	75.6
Absolute differences between pre- and post-treatment values						
ADC (0,800), 10^{-6} mm^2/s	0.648 (0.104)	0.136				
D′, 10^{-6} mm^2/s	0.747 (0.088)	**0.013**	189	96.8	50	84.4
f′	1.000* (0.000)	**<0.0001**	0.003	100	100	100
Long-term RECIST response						
Pretreatment						
ADC (0,800), 10^{-6} mm^2/s	0.585* (0.116)	0.484				
D′, 10^{-6} mm^2/s	0.606* (0.114)	0.364				
f′	0.709 (0.109)	0.073				
Post-treatment						
ADC (0,800), 10^{-6} mm^2/s	0.752 (0.095)	**0.031**	1716	60	91	73
D′, 10^{-6} mm^2/s	0.830 (0.079)	**0.005**	1707	60	100	77
f′	0.770* (0.094)	**0.021**	0.043	80	73	77
Absolute differences between pre- and post-treatment values						
ΔLD, mm	0.903* (0.058)	**0.001**	5.75	73	91	81
ΔADC (0,800), 10^{-6} mm^2/s	0.758 (0.103)	**0.027**	235	87	36	77
ΔD′, 10^{-6} mm^2/s*	0.879 (0.068)	**0.001**	403	87	73	85
Δf′	0.867* (0.089)	**0.002**	0.011	100	82	89

ADC = apparent diffusion coefficient, AUC = area under the curve, D′ = estimated true diffusion coefficient (i.e., ADC(50,800)), f′ = estimated perfusion fraction, LD = longest diameter, RECIST = response evaluation criteria in solid tumors, SE = standard error.
*Negative test direction (lower test result indicates more positive test).Significant test results given in bold.

reduction has been shown in primary colorectal cancer.[50] In contrast to these studies investigating response to systemic therapy, we did not observe significant differences in pretreatment ADC(0,800) or D′. This may be explained by a different mechanism between chemotherapy and radioembolization, as effectiveness of chemotherapy is reduced in necrotic tumors due to hypoxia and tissue acidity.[51,52] The embolizing effect of resin spheres leads to a certain degree of hypoxia anyway. However, we observed that higher pretherapeutical f′-values allowed for prediction of tumor size reduction, while prediction of RECIST response at 3 months follow-up was not possible. It is important to note, that employing RECIST criteria, the detection of new metastases lead to classification as PD in 3 cases while tumor size remained stable or decreased. Development of new metastases is unlikely to be predictable by assessing DWI data of already existing metastases.

In addition to pretherapeutical response prediction, early post-therapeutical response assessment is desirable to guide further treatment strategy (e.g., avoiding long periods of ineffective treatments, planning of further radioembolization sessions).[17,53] As morphological response evaluation is limited by tumor size changes occurring late after treatment,[1–8] functional imaging modalities have been proposed for early response assessment (e.g., mRECIST for hepatocellular carinoma[11] or PET/CT for colorectal liver metastases).[9] Radioembolization is nowadays often performed in a sequential lobar approach with an interval of 4 to 6 weeks between RE procedures, especially in patients with impaired liver function. Using conventional response criteria the second procedure would therefore be performed before therapeutic efficacy of the first radioembolization procedure could be assessed. To avoid possibly ineffective further treatment sessions, prediction of response at an earlier stage is desirable. Furthermore, in patients not responding to radioembolization, additional systemic therapy may be indicated. Early response assessment is therefore also important in order not to delay additional treatment.[53] Interestingly, DWI-derived ADC changes 6 weeks after radioembolization of liver metastases were recently shown to be of higher diagnostic value than FDG-PET.[53] Studies investigating conventional DWI for early response assessment of mBRC, however, are scarce. A significant increase in the overall ADC has been reported in mBRC patients responding to chemotherapy.[17] We also observed an ADC(0,800) increase in metastases responding to radioembolization which in general has been shown to correlate with the degree of necrosis.[3,11,13,14,16] In addition to increasing ADC(0,800) values, our analysis revealed a D′ increase in combination with an f′ decrease in metastases showing size reduction. f′ changes showed the best discriminatory power between tumor-shrinkage and -growth, while ADC(0,800) changes were not associated with size changes.

TABLE 4. Results of Group Comparison for Responders (CR, PR, and SD) and Nonresponders (PD) According to Long-Term RECIST

	Responders (n = 15)	Nonresponder (n = 11)	*P* Value
Pretreatment			
ADC (0,800), 10^{-6} mm^2/s	1221.9 ± 357.3	1227.2 ± 146.4	0.959
D′, 10^{-6} mm^2/s	1125.0 ± 312.6	1170.9 ± 170.0	0.664
f′	0.0831 ± 0.0407	0.0561 ± 0.0316	0.080
Post-treatment			
ADC (0,800), 10^{-6} mm^2/s	1702.5 ± 340.1	1397.1 ± 260.5	**0.020**
D′, 10^{-6} mm^2/s	1724.2 ± 310.6	1324.3 ± 265.2	**0.002**
f′	0.0340 ± 0.0214	0.0636 ± 0.0374	**0.032**
Absolute differences between pre- and post-treatment values			
LD changes	−7.5 ± 4.5	4.6 ± 11.6	**0.001**
ΔADC (0,800), 10^{-6} mm^2/s	480.6 ± 238.6	169.9 ± 351.7	**0.013**
ΔD′, 10^{-6} mm^2/s	599.2 ± 227.8	153.4 ± 344.6	**0.001**
Δf′	−0.0491 ± 0.0311	0.0075 ± 0.0421	**0.001**

Patients showing PD on first follow-up who died or were too ill to an attend second follow-up were also rated as nonresponders. Data are given as mean and standard deviation over the region of interest values. $P < 0.05$ considered statistically significant (2-sided Student *t* test for independent samples).

ADC = apparent diffusion coefficient, CR = complete response, D′ = estimated true diffusion coefficient (i.e., ADC(50,800)), f′ = estimated perfusion fraction, LD = longest diameter, PD = progressive disease, PR = partial response, , RECIST = response evaluation criteria in solid tumors, SD = stable disease.

Significant test results given in bold.

Our results therefore suggest that ADC(0,800) changes alone can underestimate the extend of necrosis due to counteracting perfusion changes so that a D′ increase and an f′ reduction may reflect necrosis more accurately.[3,22] The accuracy of D′ and f′ changes for prediction of RECIST response was also higher than for the conventional ADC(0,800). Interestingly the accuracy of both IVIM parameters for prediction of response was even higher than that of short-term tumor size changes.

Although DWI may have potential for early response assessment, the ideal point in time for examination after therapy remains unclear. In mBRC patients, ADC changes as early as 4 and 11 days after treatment predicted response to chemotherapy determined at 39 days.[17] Changes in perfusion-related parameters may be observed even earlier as demonstrated in an animal model treated with a vascular disrupting agent. Reduction of f- and D*-values was observed already 4 h after application, while D increased 24 h later.[54] Our data suggest that especially f′ measured 4 to 6 weeks after treatment can yield additional information about future tumor size changes. In 1 case demonstrating reduction of the LD of all metastases at first follow-up, f′-values had increased considerably after treatment. Unlike other patients showing tumor-shrinkage accompanied by an f′ decrease, this patient did not show stabilization or further shrinkage but considerable growth of the metastases on 3 months follow-up.

Interestingly, in a recent study, high preinterventional perfusion values and an early therapy-induced reduction of arterial perfusion of metastases measured by perfusion CT was found in responders after radioembolization.[10,55,56] These results seem to be in line with our findings concerning the estimated perfusion fraction f′. However, a direct comparison between the imaging methods has not yet been performed. Of note, perfusion CT has the disadvantage of a rather high radiation dose of up to 18 mSv.[56]

Our study is limited by its retrospective design associated with known inherent limitations. The study population was rather small; however, radioembolization of mBRC is not routinely performed even in tertiary referral centers but only in individual cases as a salvage therapy in otherwise therapy-refractory patients. Moreover, only patients receiving MR examinations before and after treatment using the same protocol could be included. Classification of tumor response was performed on the basis of tumor size changes within the first 3 months after treatment. In most of the nonresponders, diameter measurements derived from first follow-up imaging had to be used as many of these patients did not survive or were unable to attend the second follow-up examination due to severe illness. It is important to note that in our small patient group we observed an early change in tumor size in a rather large percentage of cases so that also tumor size changes alone predicted response with fair accuracy. Utility of IVIM parameters may even be greater in a cohort showing only late tumor size changes. Although the results of response assessment using IVIM DWI are compelling, further prospective studies, especially on reproducibility of the employed simplified IVIM approach and the ideal point in time to perform early DWI follow-up are warranted before clinical use of these parameters can be recommended. Furthermore, the impact of an early change of treatment strategy guided by early response criteria has so far not been assessed.

In conclusion, our study showed that a simplified IVIM model-based analysis of DWI obtained 4 to 6 weeks after treatment can deliver additional information on long-term tumor size changes and RECIST response after radioembolization of mBRC, which can be useful to guide further treatment strategy. While pretherapeutic f′-values may predict post-therapeutic tumor size changes, RECIST response could not be predicted pretherapeutically, probably because the development of new metastases cannot be foreseen by analyzing the properties of existing tumor tissue. The estimated perfusion fraction f′ seems to be better suited to assess response than the conventional ADC(0,800), D′ or tumor size changes. A therapy-induced change in f′ may be a potential biomarker for accurate and early prediction of tumor size changes and RECIST response.

REFERENCES

1. Eisenhauer EA, Therasse P, Bogaerts J, et al. New response evaluation criteria in solid tumours: revised RECIST guideline (version 1.1). *Eur J Cancer.* 2009;45:228–247.
2. Li SP, Padhani AR. Tumor response assessments with diffusion and perfusion MRI. *J Magn Reson Imaging.* 2012;35:745–763.
3. Thoeny HC, Ross BD. Predicting and monitoring cancer treatment response with diffusion-weighted MRI. *J Magn Reson Imaging.* 2010;32:2–16.
4. Husband JE, Schwartz LH, Spencer J, et al. Evaluation of the response to treatment of solid tumours—a consensus statement of the International Cancer Imaging Society. *Br J Cancer.* 2004;90:2256–2260.
5. Kennedy AS, Salem R. Radioembolization (yttrium-90 microspheres) for primary and metastatic hepatic malignancies. *Cancer J.* 2010;16:163–175.
6. Bester L, Hobbins PG, Wang S-C, et al. Imaging characteristics following 90yttrium microsphere treatment for unresectable liver cancer. *J Med Imaging Radiat Oncol.* 2011;55:111–118.
7. Bienert M, McCook B, Carr BI, et al. 90Y microsphere treatment of unresectable liver metastases: changes in ^{18}F-FDG uptake and tumour size on PET/CT. *Eur J Nucl Med Mol Imaging.* 2005;32:778–787.
8. Szyszko T, Al-Nahhas A, Canelo R, et al. Assessment of response to treatment of unresectable liver tumours with 90Y microspheres: value of FDG PET versus computed tomography. *Nucl Med Commun.* 2007;28:15–20.
9. Sabet A, Meyer C, Aouf A, et al. Early post-treatment FDG PET predicts survival after (90)Y microsphere radioembolization in liver-dominant metastatic colorectal cancer. *Eur J Nucl Med Mol Imaging.* 2015;42:370–376.
10. Morsbach F, Sah B-R, Spring L, et al. Perfusion CT best predicts outcome after radioembolization of liver metastases: a comparison of radionuclide and CT imaging techniques. *Eur Radiol.* 2014;24:1455–1465.
11. Vandecaveye V, Michielsen K, De Keyzer F, et al. Chemoembolization for hepatocellular carcinoma: 1-month response determined with apparent diffusion coefficient is an independent predictor of outcome. *Radiology.* 2014;270:747–757.
12. Dudeck O, Zeile M, Wybranski C, et al. Early prediction of anticancer effects with diffusion-weighted MR imaging in patients with colorectal liver metastases following selective internal radiotherapy. *Eur Radiol.* 2010;20:2699–2706.
13. Chiaradia M, Baranes L, Van Nhieu JT, et al. Intravoxel incoherent motion (IVIM) MR imaging of colorectal liver metastases: are we only looking at tumor necrosis? *J Magn Reson Imaging.* 2014;39:317–325.
14. Padhani AR, Koh DM. Diffusion MR imaging for monitoring of treatment response. *Magn Reson Imaging Clin N Am.* 2011;19:181–209.
15. Padhani AR, Liu G, Koh DM, et al. Diffusion-weighted magnetic resonance imaging as a cancer biomarker: consensus and recommendations. *Neoplasia.* 2009;11:102–125.
16. Koh DM, Collins DJ. Diffusion-weighted MRI in the body: applications and challenges in oncology. *Am J Roentgenol.* 2007;188:1622–1635.
17. Theilmann RJ, Borders R, Trouard TP, et al. Changes in water mobility measured by diffusion MRI predict response of metastatic breast cancer to chemotherapy. *Neoplasia.* 2004;6:831–837.
18. Heijmen L, ter Voert EEGW, Oyen WJG, et al. Multimodality imaging to predict response to systemic treatment in patients with advanced colorectal cancer. *PLoS ONE.* 2015;10:http://www.ncbi.nlm.nih.gov/pmc/articles/PMC4382283/. Accessed September 18, 2015.
19. Le Bihan D, Breton E, Lallemand D, et al. Separation of diffusion and perfusion in intravoxel incoherent motion MR imaging. *Radiology.* 1988;168:497–505.
20. Koh DM, Collins DJ, Orton MR. Intravoxel incoherent motion in body diffusion-weighted MRI: reality and challenges. *Am J Roentgenol.* 2011;196:1351–1361.
21. Kukuk GM, Mürtz P, Träber F, et al. Diffusion-weighted imaging with acquisition of three b-values for response evaluation of neuroendocrine liver metastases undergoing selective internal radiotherapy. *Eur Radiol.* 2014;24:267–276.
22. Lewin M, Fartoux L, Vignaud A, et al. The diffusion-weighted imaging perfusion fraction f is a potential marker of sorafenib treatment in advanced hepatocellular carcinoma: a pilot study. *Eur Radiol.* 2011;21:281–290.
23. ter Voert EEGW, Delso G, Porto M, et al. Intravoxel incoherent motion protocol evaluation and data quality in normal and malignant liver tissue and comparison to the literature. *Invest Radiol.* 2015. DOI: 10.1097/RLI.0000000000000207. http://www.ncbi.nlm.nih.gov/pubmed/26405835.
24. Cohen AD, Schieke MC, Hohenwalter MD, et al. The effect of low b-values on the intravoxel incoherent motion derived pseudodiffusion parameter in liver. *Magn Reson Med.* 2015;73:306–311.
25. Leporq B, Saint-Jalmes H, Rabrait C, et al. Optimization of intravoxel incoherent motion imaging at 3.0 Tesla for fast liver examination. *J Magn Reson Imaging.* 2015;41:1209–1217.
26. Chung SR, Lee SS, Kim N, et al. Intravoxel incoherent motion MRI for liver fibrosis assessment: a pilot study. *Acta Radiol.* 2014DOI:10.1177/0284185114559763. http://acr.sagepub.com/content/early/2014/11/20/0284185114559763.
27. Guiu B, Petit JM, Capitan V, et al. Intravoxel incoherent motion diffusion-weighted imaging in nonalcoholic fatty liver disease: a 3.0-T MR study. *Radiology.* 2012;265:96–103.
28. Luciani A, Vignaud A, Cavet M, et al. Liver cirrhosis: intravoxel incoherent motion MR imaging—pilot study. *Radiology.* 2008;249:891–899.
29. Kakite S, Dyvorne H, Besa C, et al. Hepatocellular carcinoma: short-term reproducibility of apparent diffusion coefficient and intravoxel incoherent motion parameters at 3.0T. *J Magn Reson Imaging.* 2015;41:149–156.
30. Woo S, Lee JM, Yoon JH, et al. Intravoxel incoherent motion diffusion-weighted MR imaging of hepatocellular carcinoma: correlation with enhancement degree and histologic grade. *Radiology.* 2014;270:758–767.
31. Andreou A, Koh DM, Collins DJ, et al. Measurement reproducibility of perfusion fraction and pseudodiffusion coefficient derived by intravoxel incoherent motion diffusion-weighted MR imaging in normal liver and metastases. *Eur Radiol.* 2013;23:428–434.
32. Lee JT, Liau J, Murphy P, et al. Cross-sectional investigation of correlation between hepatic steatosis and IVIM perfusion on MR imaging. *Magn Reson Imaging.* 2012;30:572–578.
33. Cho GY, Kim S, Jensen JH, et al. A versatile flow phantom for intravoxel incoherent motion MRI. *Magn Reson Med.* 2012;67:1710–1720.
34. Lemke A, Stieltjes B, Schad LR, et al. Toward an optimal distribution of b values for intravoxel incoherent motion imaging. *Magn Reson Imaging.* 2011;29:766–776.
35. Kennedy A, Nag S, Salem R, et al. Recommendations for radioembolization of hepatic malignancies using yttrium-90 microsphere brachytherapy: a consensus panel report from the radioembolization brachytherapy oncology consortium. *Int J Radiat Oncol Biol Phys.* 2007;68:13–23.

36. Mahnken AH, Spreafico C, Maleux G, et al. Standards of practice in transarterial radioembolization. *Cardiovasc Intervent Radiol.* 2013;36:613–622.
37. Concia M, Sprinkart AM, Penner A-H, et al. Diffusion-weighted magnetic resonance imaging of the pancreas: diagnostic benefit from an intravoxel incoherent motion model-based 3 b-value analysis. *Invest Radiol.* 2014;49:93–100.
38. Penner A-H, Sprinkart AM, Kukuk GM, et al. Intravoxel incoherent motion model-based liver lesion characterisation from three b-value diffusion-weighted MRI. *Eur Radiol.* 2013;23:2773–2783.
39. Koh DM. Science to practice: can intravoxel incoherent motion diffusion-weighted MR imaging be used to assess tumor response to antivascular drugs? *Radiology.* 2014;272:307–308.
40. Yamada I, Aung W, Himeno Y, et al. Diffusion coefficients in abdominal organs and hepatic lesions: evaluation with intravoxel incoherent motion echo-planar MR imaging. *Radiology.* 1999;210:617–623.
41. Lee HJ, Rha SY, Chung YE, et al. Tumor perfusion-related parameter of diffusion-weighted magnetic resonance imaging: correlation with histological microvessel density. *Magn Reson Med.* 2014;71:1554–1558.
42. Bauerle T, Seyler L, Munter M, et al. Diffusion-weighted imaging in rectal carcinoma patients without and after chemoradiotherapy: a comparative study with histology. *Eur J Radiol.* 2013;82:444–452.
43. Kim S, Decarlo L, Cho GY, et al. Interstitial fluid pressure correlates with intravoxel incoherent motion imaging metrics in a mouse mammary carcinoma model. *NMR Biomed.* 2012;25:787–794.
44. Gade TP, Buchanan IM, Motley MW, et al. Imaging intratumoral convection: pressure-dependent enhancement in chemotherapeutic delivery to solid tumors. *Clin Cancer Res.* 2009;15:247–255.
45. Wagner M, Doblas S, Daire JL, et al. Diffusion-weighted MR imaging for the regional characterization of liver tumors. *Radiology.* 2012;264:464–472.
46. Tam HH, Collins DJ, Brown G, et al. The role of pre-treatment diffusion-weighted MRI in predicting long-term outcome of colorectal liver metastasis. *Br J Radiol.* 2013;86:1–8.
47. Lee Y, Lee SS, Kim N, et al. Intravoxel incoherent motion diffusion-weighted MR imaging of the liver: effect of triggering methods on regional variability and measurement repeatability of quantitative parameters. *Radiology.* 2015;274:405–415.
48. Lemke A, Laun FB, Simon D, et al. An in vivo verification of the intravoxel incoherent motion effect in diffusion-weighted imaging of the abdomen. *Magn Reson Med.* 2010;64:1580–1585.
49. Cui Y, Zhang XP, Sun YS, et al. Apparent diffusion coefficient: potential imaging biomarker for prediction and early detection of response to chemotherapy in hepatic metastases. *Radiology.* 2008;248:894–900.
50. Dzik-Jurasz A, Domenig C, George M, et al. Diffusion MRI for prediction of response of rectal cancer to chemoradiation. *Lancet.* 2002;360:307–308.
51. Trédan O, Galmarini CM, Patel K, et al. Drug resistance and the solid tumor microenvironment. *J Natl Cancer Inst.* 2007;99:1441–1454.
52. Brown JM. The hypoxic cell: a target for selective cancer therapy—eighteenth Bruce F. Cain Memorial Award lecture. *Cancer Res.* 1999;59:5863–5870.
53. Barabasch A, Kraemer NA, Ciritsis A, et al. Diagnostic accuracy of diffusion-weighted magnetic resonance imaging versus positron emission tomography/computed tomography for early response assessment of liver metastases to Y90-radioembolization. *Invest Radiol.* 2015DOI:10.1097/rli.0000000000000144. http://www.ncbi.nlm.nih.gov/pubmed/25763526.
54. Joo I, Lee JM, Han JK, et al. Intravoxel incoherent motion diffusion-weighted MR imaging for monitoring the therapeutic efficacy of the vascular disrupting agent CKD-516 in rabbit VX2 liver tumors. *Radiology.* 2014;272:417–426.
55. Morsbach F, Pfammatter T, Reiner CS, et al. Computed tomographic perfusion imaging for the prediction of response and survival to transarterial radioembolization of liver metastases. *Invest Radiol.* 2013;48:787–794.
56. Reiner CS, Morsbach F, Sah B-R, et al. Early treatment response evaluation after Yttrium-90 radioembolization of liver malignancy with CT perfusion. *J Vasc Interv Radiol.* 2014;25:747–759.